Revista Brasileira de Meteorologia, **v. 38,** e38230017, 2023
DOI: http://dx.doi.org/10.1590/0102-77863810017 rbmet.org.br

Artigo

Assessment of Precipitation Deficit in the São Francisco River Basin From 1998 to 2018

José H.B. Damasceno[1], Erick V.S.V. Oliveira[1], Fábio Farias Pereira[1#], Zheng Duan[2#]

[1]*Campus de Engenharias e Ciências Agrárias, Universidade Federal de Alagoas, Rio Largo, AL, Brazil.*
[2]*Department of Physical Geography and Ecosystem Science, Lund University, Lund, Sweden.*

Recebido em: 4 de Outubro de 2022 - Aceito em: 4 de Novembro de 2022

Resumo

Este trabalho apresenta uma avaliação do déficit de precipitação na Bacia Hidrográfica do Rio São Francisco (SFRB) com base em análises temporais, sazonais e regionais de duas décadas de produtos de dados de precipitação derivados de missões de satélite lançadas desde 1997. As análises temporais foram realizadas por meio de três Série temporal SPI de 3 meses, composta por 250 valores cada, derivados de estimativas TRMM, CHIRPS e PERSIANN-CDR. Análises sazonais e regionais foram feitas com diferenças nas quantidades médias de precipitação entre a última década, abrangendo de janeiro de 2008 a dezembro de 2018, e a década anterior, abrangendo de janeiro de 1998 a dezembro de 2007, para cada célula da grade no domínio do SFRB. O resultado da análise temporal mostra que o SFRB passou por períodos mais longos e mais secos na década 2008-2018. Os resultados das análises sazonais e regionais sugerem que o défice de precipitação foi mais forte durante o verão; e que a parte superior do SFRB foi a mais impactada pelo déficit de precipitação ocorrido nas últimas duas décadas.

Palavras-chave: Semiárido brasileiro, dados de satélite, SPI, déficit hídrico.

Avaliação do Déficit de Precipitação na Bacia Hidrográfica do Rio São Francisco de 1998 a 2018

Abstract

This work presents an assessment of the precipitation deficit in the São Francisco River Basin (SFRB) based on temporal, seasonal and regional analyses of two decades of precipitation data products derived from satellite missions launched since 1997. The temporal analyses were performed by means of three 3-month SPI time series, consisting of 250 values each derived from TRMM, CHIRPS and PERSIANN-CDR estimates. Seasonal and regional analyses were made with differences in precipitation amounts averaged between the last decade, spanning from January 2008 to December 2018, and the decade before that one, spanning from January 1998 to December 2007, for each grid cell over the domain of the SFRB. The result from the temporal analysis shows that the SFRB experienced longer and drier periods in the decade 2008-2018. The results of the seasonal and regional analyses suggest that precipitation deficit was stronger during the summer; and that the upper part of the SFRB was the most impacted by the precipitation deficit occurred over the past two decades.

Keywords: Brazilian semiarid, satellite-derived data, SPI, water deficit.

1. Introduction

São Francisco River is the largest Brazilian river that flows entirely within the country, with much of its drainage area being in arid and semi-arid regions under threat from frequent droughts. Estimates of consumptive water uses (by hydrological region) for the country reveal an increase of 73% in water withdrawals for irrigation from 2006 to 2010 in the São Francisco River alone (ANA,

Corresponding author: Fábio Farias Pereira. E-mail: fabio.pereira@ceca.ufal.br.
#These authors contributed equally to this work.

2013). Maneta *et al.* (2009a) demonstrated how co-cultivation and production technologies could reduce water use for agriculture, but improved agriculture practices are more labor and knowledge intensive and the overall costs of adjustments in cultivation and improved technologies for higher production are beyond the reach of poor farmers (Hazell and Wood, 2008).

Domestic water use is also expected to increase in the following decades in the São Francisco River basin because it is home to Brazil's major water diversion project, the Projeto de Integração do rio São Francisco (PISF), which aims to deliver São Francisco River water into temporary streams, lakes and ponds in the states of Pernambuco, Paraíba, Ceará and Rio Grande do Norte through two major canals of 260 km and 217 km. Altogether it is reckoned that the project would provide domestic water to nearly 12 million people living in 390 counties over semiarid lands in the North-Eastern Region of Brazil (NERB) (BRASIL, 2004). The PISF construction work started in 2005 and the canals are about to become fully operational.

Apart of the consumptive water uses, there are 12 dams in the São Francisco River basin operated by Companhia Hidro Elétrica do São Francisco (Chesf), the subsidiary of the eletricity corporation Centrais Elétricas Brasileiras S.A. (a.k.a. Eletrobras) who operates in the sectors of generation, transmission and distribution of electrical energy in Brazil, with 8 of the 12 dams in the main stem of the river. All the 12 dams provide many tens of gigawatts of power to the National

Interconnected System (NIS) (Chesf, 2020). However, given the current pace at which rainfall has decreased over the São Francisco River basin, de Jong *et al.* (2018) pointed out that the share of wind and solar power to the NIS will need to significantly increase to catch-up with the loss of hydroelectric power due to the projected decrease in rainfall by 2100.

For all of these reasons, several studies have investigated the components of the hydrologic cycle in the São Francisco River basin (Santos and de Morais, 2013; Souto *et al.*, 2019; De Paiva *et al.*, 2020; Ferreira *et al.*, 2021; Lucas *et al.*, 2021); how they would respond to climate change (Marengo *et al.*, 2012; Bezerra *et al.*, 2019; da Silva *et al.*, 2021), to different scenarios of irrigation (Maneta *et al.*, 2009b), and to frequent droughts (Trejo *et al.*, 2016; Santos *et al.*, 2017); and what would that mean to the water availability in the basin (Torres *et al.*, 2012; Sun *et al.*, 2016; Alves da Silva Rosa *et al.*, 2021; Coutinho and Cataldi, 2021; Lucas *et al.*, 2021). Clearly, the amount of precipitation and its variability over time are key drivers of water availability in the São Francisco River basin. Trejo *et al.* (2016) used rainfall data of 41 rain gauge stations from the Instituto Nacional de Meteorologia (INMET) database to investigate the patterns of the dry periods in the São Francisco River basin from 1961 to 2010. Their analysis identified a moderate seasonality of droughts in the basin, as the drought events were more frequent during October-November and January-March. Evidences of the influence of the tropical Atlantic and Pacific Oceans on dry spells have also been reported in Northeast region of Brazil (NEB), where most of the São Francisco River basin lies (Andreoli and Kayano, 2007; Rodrigues *et al.*, 2011; Kayano and Andreoli, 2006).

A succession of satellite-borne instruments has been launched since the 1970s, with the Tropical Rainfall Measuring Mission (launched in 1997) being the first to bring a precipitation radar, a spaceborne instrument designed to provide 3D maps of storm structure, into orbit. All sorts of analysis of precipitation over the tropics using its database (and the database of its successors) have systematically been published ever since, as in Su *et al.* (2008); Oliveira *et al.* (2014); Santos *et al.* (2017, 2018); Brasil Neto *et al.* (2021), to list only those in the São Francisco River basin and its surroundings. Away from the São Francisco River basin, other two rainfall data set are commonly used to explore drought patterns at large scale: the Climate Hazards Group InfraRed Precipitation with Station data (CHIRPS) (Gao *et al.*, 2018a; Mun et al, 2019; Sandeep *et al.*, 2021) and the Precipitation Estimation from Remotely Sensed Information using Artificial Neural Networks - Climate Data Record (PERSIANN-CDR) (Santos *et al.*, 2021; Alijanian *et al.*, 2022; Lai *et al.*, 2019). Out of all these studies, the ones using the Standard Precipitation Index (SPI) stand out as being a worldwide indicator for detecting and classifying droughts as it is based on the probability of a single variable: the precipitation itself.

As the time passed since the first mission was launched in 1997, we can now propose more robust temporal analysis of precipitation for the tropical and sub-tropical regions of the Earth using the database of the Global Precipitation Measurement (GPM) mission, an international network of satellites that provide next-generation global observations of precipitation, which was built upon the success of the Tropical Rainfall Measuring Mission (TRMM). Estimates of precipitation from the GPM span the period from December 1997 to present and cover entirely the São Francisco River basin.

Estimates of precipitation from TRMM, PERSIANN-CDR and CHIRPS have been used to respond to the concern raised by this research, which is: whether there was a precipitation deficit in the São Francisco River basin over the past two decades. To answer this question, this work presents a multi-decadal analysis of precipitation deficit as differences of monthly precipitation totals and how monthly precipitation totals deviate from the long-term precipitation mean over the São Francisco River basin. We hypothesize that precipitation deficit was greater in the last decade (2008-2018) - which, for simplicity, will be referred as D2 - than the decade before that one (1998-2008) - which will be referred as D1 - during the summers, resulting to drier summers across the basin through the 2008-2018 period. But would this precipitation deficit have been partly compensated with precipitation excess over the other seasons of the year, making the annual precipitation total remain constant? If not, could regional patterns in precipitation deficit to be linked to the decrease (or increase) trend in annual precipitation totals over the basin?

2. Methods

For this work, we used estimates of precipitation from satellite data products to investigate the droughts occurred in the São Francisco River basin (SFRB) from 1998 (beginning of measurements) to 2018. For planning purposes (of governmental and non-governmental actions), São Francisco River basin is commonly divided into four parts: Upper, Middle, Lower Middle and Lower parts. Roughly 54% of its drainage area belongs to the Brazilian Semiarid region, which is characterized by frequent, intense, and longer lasting droughts (see Fig. 1).

2.1. Monthly precipitation in the SFRB

We extracted monthly precipitation totals from the three following satellite products: TRMM 3B43, PERSIANN-CDR and CHIRPS. The TRMM 3B43 (TRMM) algorithm merges daily data from passive microwave and precipitation radar sensors on board the Tropical Rainfall Measuring Mission (TRMM) satellite at a spatial resolution of 0.25 degrees. The PERSIANN-CDR algorithm combines data from infrared and passive microwave from multiple geostationary satellites from the International Satellite Cloud Climatology Project (ISCCP) at a spatial resolution of 0.25 degrees (PERSIANN-CDR). The CHIRPS algorithm retrieves its estimates of precipitation from global infrared Cold Cloud Duration observations at a spatial resolution of 0.05 degrees. It is important to note that CHIRPS estimates of precipitation were calibrated with one of the Tropical Rainfall Measuring Mission (TRMM) products, the TRMM 3B42 algorithm.

2.2. 3-month SPI time series

We computed the Standardized Precipitation Index (SPI) to evaluate how far monthly precipitation totals deviate from the long-term precipitation mean and used it as a measure of the precipitation deficit in the São Francisco River basin (SFRB). The monthly precipitation totals consisted of averaging out monthly means of TRMM, PERSIANN and CHIRPS datasets for each of their grid points, individually and separately. Then, the values of SPI were obtained by fitting the monthly precipitation totals from each satellite product to a gamma distribution (Cho *et al.*, 2004).

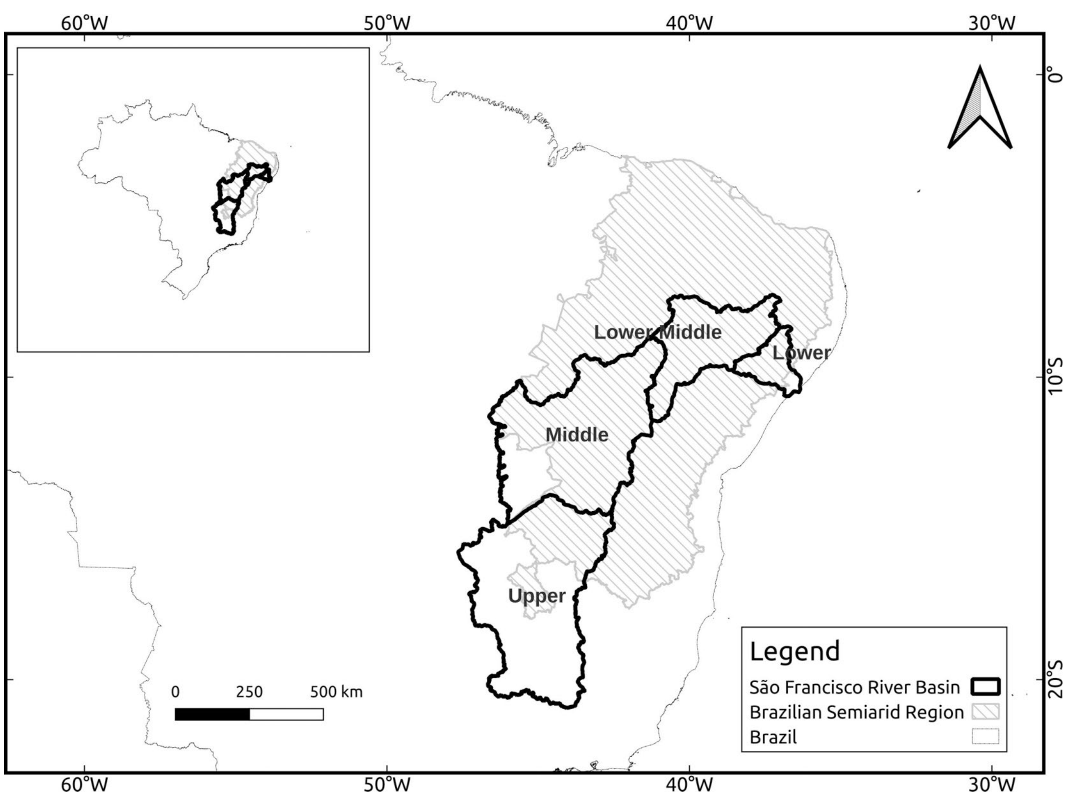

Fig. 1 - The study area of the drought assessment outlined in this work: The São Francisco River basin (and its parts). Also, we included a contour for the Brazilian Semiarid region, as part of results refers to it.

Because we used values of SPI to investigate the precipitation deficit, which is a predictive indicator of surface water availability, we computed the SPI values for the period of 3-months. For groundwater and reservoir storage applications (i.e. applications that require longer hydrologic memory), the periods of 6-to-48 months are recommended instead (Esit *et al.*, 2021). Thus, 3-month SPI time series were created from gridded monthly precipitation totals averaged over the SFRB for a 20-year period, spanning from January 1998 to December 2018, for each of the three satellite products. After that, we assumed that the precipitation deficit occurred when the overall cumulative probability for 3-month SPI values fell below 15 % of cases (i.e. for the cases when 3-month SPI values are less than or equal to -1.0) considering the three satellite products, in this way we cross-validated the periods in which precipitation deficit occurred. Then, we used the non-parametric Mann-Kendall (MK) statistical test to assess the trend in all the 3-month SPI time series, at the significance level of 0.05, with the null hypothesis (H_0) that there is no trend present in the time series.

2.3. Seasonal and regional analyses

Additionally, to the analysis of the values of 3-month SPI, our drought assessment also includes investigating differences in monthly precipitation totals in order to identify seasonal and regional changes in precipitation deficit in the SFRB. So, differences in monthly precipitation totals between D2 and D1 were computed. First, monthly precipitation totals were averaged for each of the two decades, then we calculated the differences in precipitation totals for each month of the year. Here, we assumed that precipitation deficit occurred for all the months of the year in which the differences in monthly precipitation totals were negative. These computations were made for each grid cell, so we could also use this result to identify regional patterns in precipitation deficit in the SFRB. Once precipitation deficit was determined, we used the function “levelplot” of the R package “lattice” (version 0.20-45) to draw false colors level plots. The seasonal analysis in precipitation deficit was made relative to the annual cycle of precipitation in the SFRB (as from rainfall estimates of TRMM, PERSIANN and CHIRPS).

Lastly, we examined whether the precipitation deficit in SFRB is linked to ocean forcings. The effects of the tropical Pacific Ocean on the precipitation deficit in the SFRB are evaluated with the 3-month running mean of sea surface temperature anomalies from the Extended Reconstructed Sea Surface Temperature (ERSSTv5) in the Niño 3.4 region (5° N-5° S, 120° W-170° W), based on centered 30-year base periods updated every 5 years, widely known as the Oceanic Niño Index (ONI). The interhemispheric SSTA GRADient (GRAD), which refers to the difference of the Tropical Southern Atlantic anomaly SST index (TSA) from the Tropical Northern Atlantic anomaly SST index (TNA), have been used to indicate whether the tropical Atlantic Ocean affect the precipitation deficit in the SFRB. We used GRAD instead of TNA and TSA because it has been reported that GRAD is strongly associated with the precipitation seasonality in the Northeast Brazil (NNEB) (De Souza *et al.*, 2005; Andreoli and Kayano, 2007; Marques and Oyama, 2015; de Medeiros *et al.*, 2020).

The time series of ONI, TSA and TNA were extracted from the NOAA Physical Sciences Laboratory (PSL) database.

3. Results

3.1. The annual cycle of precipitation in the SFRB

The annual cycle of precipitation in the SFRB is presented in the form of boxplots (see Fig. 2). The boxes are limited to the first and third quartile of the precipitation data from the three satellite products for the 1998-2018 period. One could use the accumulated rainfall to classify the annual cycle of precipitation in the SFRB into dry and wet periods. The dry periods can be defined as the period in which accumulated rainfall does not exceed 50 mm per month and wet periods as the period in which they do. Based on this classification, the dry period starts in May and finishes in September, whereas the wet period spans from November to March, with April (and October) being the transition from wet to dry (and dry from wet) periods in the SFRB (Fig. 3). The seasonal analysis in precipitation deficit presented in this drought assessment used this criterion.

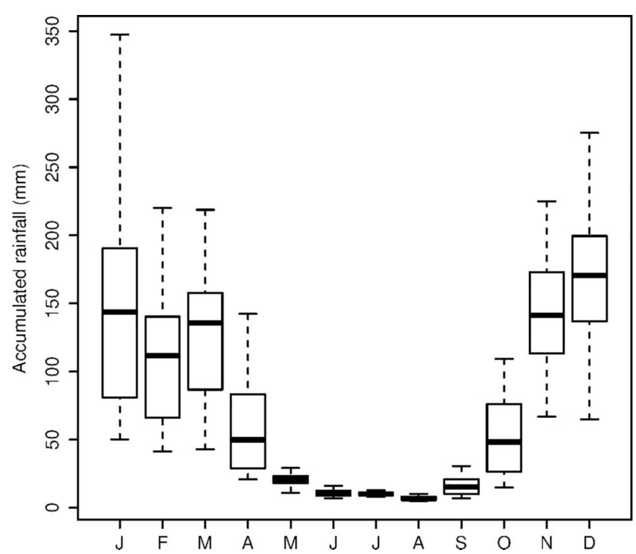

Fig. 2 - The annual cycle of precipitation in the SFRB as from estimates of rainfall from TRMM, PERSIANN and CHIRPS over the period spanning from January 1998 to December 2018.

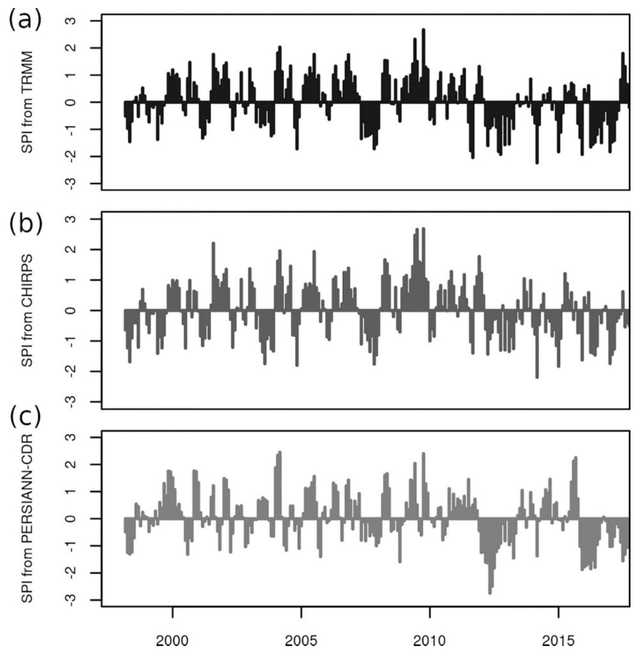

Fig. 3 - Differences in precipitation totals (in mm) between the decade 1998-2008 and the decade the decade 2008-2018 for each month of the year for the SFRB.

3.2. 3-month SPI time series

We computed 250 values of 3-month SPI for the 20-year period, ranging from January 1998 to December 2018, using the estimates of all the three satellite products separately, which resulted to three time series of values of 3-month SPI - one for each satellite product. A total of 22, 18 and 10 (for TRMM, PERSIANN-CDR and CHIRPS, respectively) out of the 250 values of SPI were below -1.0, the drought threshold set in section 2. This means that there were 10 months over the past 20 years in which the precipitation for a period of 3 months fell below 15% of the occurrences for CHIRPS; and 22 and 18 months for TRMM and for PERSIANN-CDR, respectively. The reason for this difference of SPI values from CHIRPS and the other two satellite products - roughly two-fold - could be due to the interpolation techniques used by CHIRPS to increase its spatial resolution, which could lead to smoother transitions in precipitation gradients over the SFRB (Su *et al.*, 2008; Gao *et al.*, 2018b). Also estimates from CHIRPS have proven to be underestimated over arid and semi-arid areas, where the average precipitation is small. On the other hand, estimates from TRMM have shown to have overestimated the amount of precipitation over the same arid and semi-arid areas (Zhong *et al.*, 2019). For the analysis of 3-month SPI values, we refer to the results derived from estimates of precipitation from TRMM and PERSIANN-CDR because estimates of precipitation from CHIRPS are a product of TRMM (among others satellite products and data) that were resampled to a 0.05 grid (Funk *et al.*, 2015) and the occurrence of 3-month SPI values on the range of precipitation deficit were far from those determined with estimates from the other two satellite products. Despite the differences in the number of occurrences of 3-month SPI values on the range of precipitation deficit, there is very little mismatching of the overall timing of dry periods (represented by negative values in the 3-month SPI time series in Fig. 4) for all of the three satellite products, which suggests that we could use estimates from all three satellite products for the analysis of the decadal changes in seasonal patterns of precipitation deficit in section 3.3.

The 3-month SPI time series derived from TRMM and PERSIANN-CDR estimates indicated longer periods of negative values of 3-month SPI for D2 (compared to D1). It is also when 3-month SPI values reach to -2, suggesting that dry periods became not only longer but also drier, judging by the areas in red in Fig. 4 after the year 10. In total, there were 22 and 18 periods in which SFRB was in precipitation deficit between 1998 and 2018, of which 14 and 7 periods occurred after 2008 for the 3-month SPI time series from TRMM and PERSIANN-CDR estimates, respectively. However, for all the 3-month SPI time series the precipitation deficit became severe (i.e. given by values of 3-month SPI less than -2) in the decade starting from 2008.

Another aspect that is important to point out is the number of periods in which 3-month SPI values are positive (areas in above 0 in Fig. 4). They represent the periods in which monthly precipitation totals are above the long-

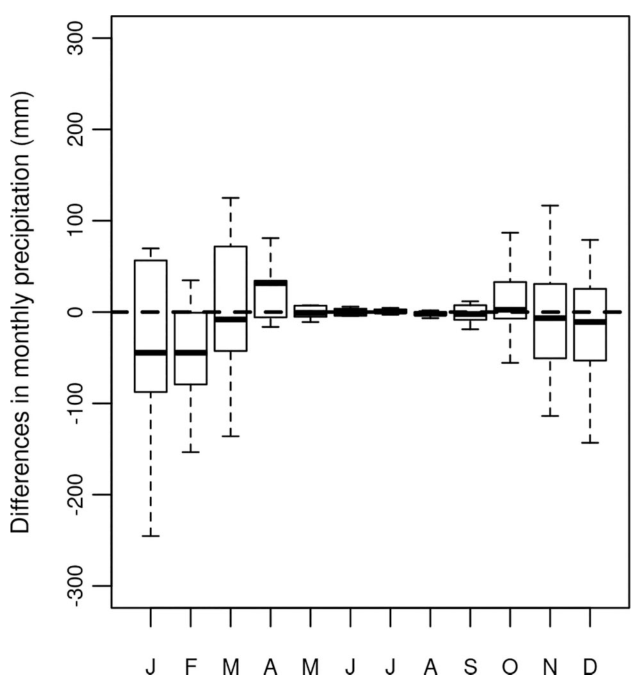

Fig. 4 - Values of 3-month SPI as calculated from estimates of monthly precipitation from the three satellite products: a) TRMM; b) CHIRPS; c) PERSSIAN-CDR.

term precipitation mean, resulting to precipitation excess. Periods of precipitation excess could be thought of as periods that would ease the impacts of the precipitation deficit in the SFRB. Figure 3 shows fewer periods of precipitation excess for D2.

A summary of the results of the MK test in all three SPI time series is presented in Table 1. The MK statistic (S), which accounts for the number of positive differences minus the number of negative differences in the MK test, is negative for all the three SPI time series. This means that values of 3-month SPI values calculated for later in the time series tend to be smaller than those for earlier. The MK test indicated that there is statistically significant evidence to reject the null hypothesis (H_0) for SPI values from TRMM and PERSIANN. Given that the metric S is below 0, one can state that there is a negative trend in the time series of SPI values from TRMM and PERSIANN. Despite the metric S is also below 0 for the SPI time series from CHIRPS, there is evidence to accept the null hypothesis (H_0), which means that no trend was detected at 5% significance level.

3.3. Seasonal and regional analyses

Seasonal and regional analyses of precipitation deficit are presented in terms of differences in precipitation totals averaged over D1 and D2 for the SFRB. Figure 5 shows the differences in precipitation totals computed for every month of the year.

Our seasonal analyses start by pointing out that differences in precipitation totals are less than 10 mm for

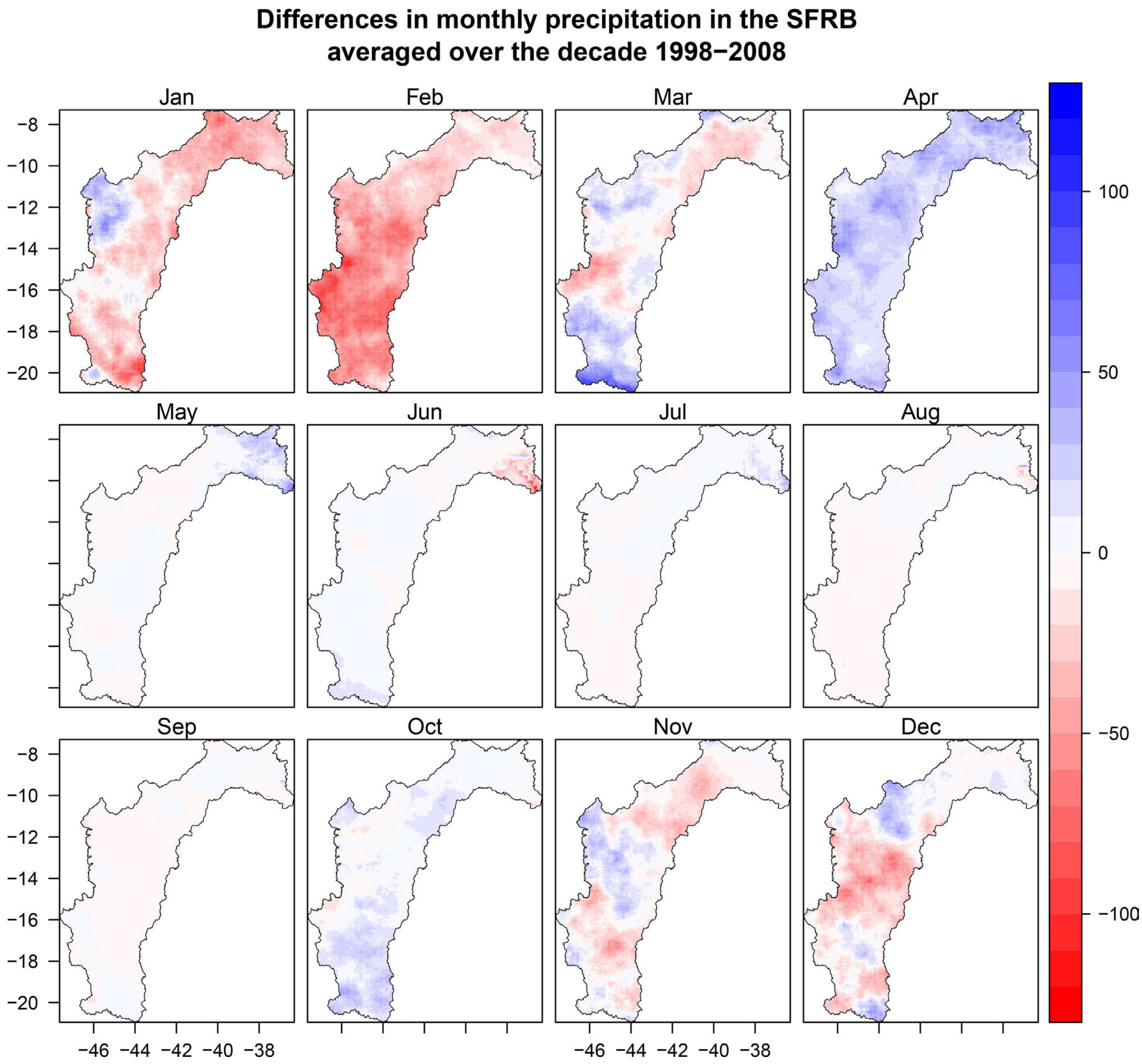

Fig. 5 - Differences in precipitation totals from CHIRPS between D1 and D2 averaged over the São Francisco River Basin.

Table 1 - Results of the Mann-Kendall test for 3-month SPI values.

	Mann-Kendall Statistic (S)	p-value (two tailed test)	Test interpretation
PERSIANN-CDR	-3809	0.00396	Reject H_0
TRMM	-3797	0.00407	Reject H_0
CHIRPS	-2077	0.09085	Accept H_0

each of the following months: May, June, July, August, September and October; suggesting that decadal changes in precipitation totals are marginal over the past two decades for them. These months encompass almost three seasons of the year: autumn (Mar 1st to May 31st), winter (Jun 1st to Aug 31st) and spring (Sep 1st to Nov 30th) in the Southern Hemisphere. So, one can summarize the seasonal analyses of changes in precipitation totals in the SFRB with the changes that occurred in the summer (Dec 1st to Feb 28th), in the beginning of autumn and the end of the spring. For the same reason, we also summarize the regional analyses of changes in precipitation totals with the changes that occurred in the same period only.

Figure 5 reveals a systematic decrease in precipitation totals already in November, the last month of spring, indicating that the period of low precipitation amount has been anticipated by one month from D1 to D2. Absolute

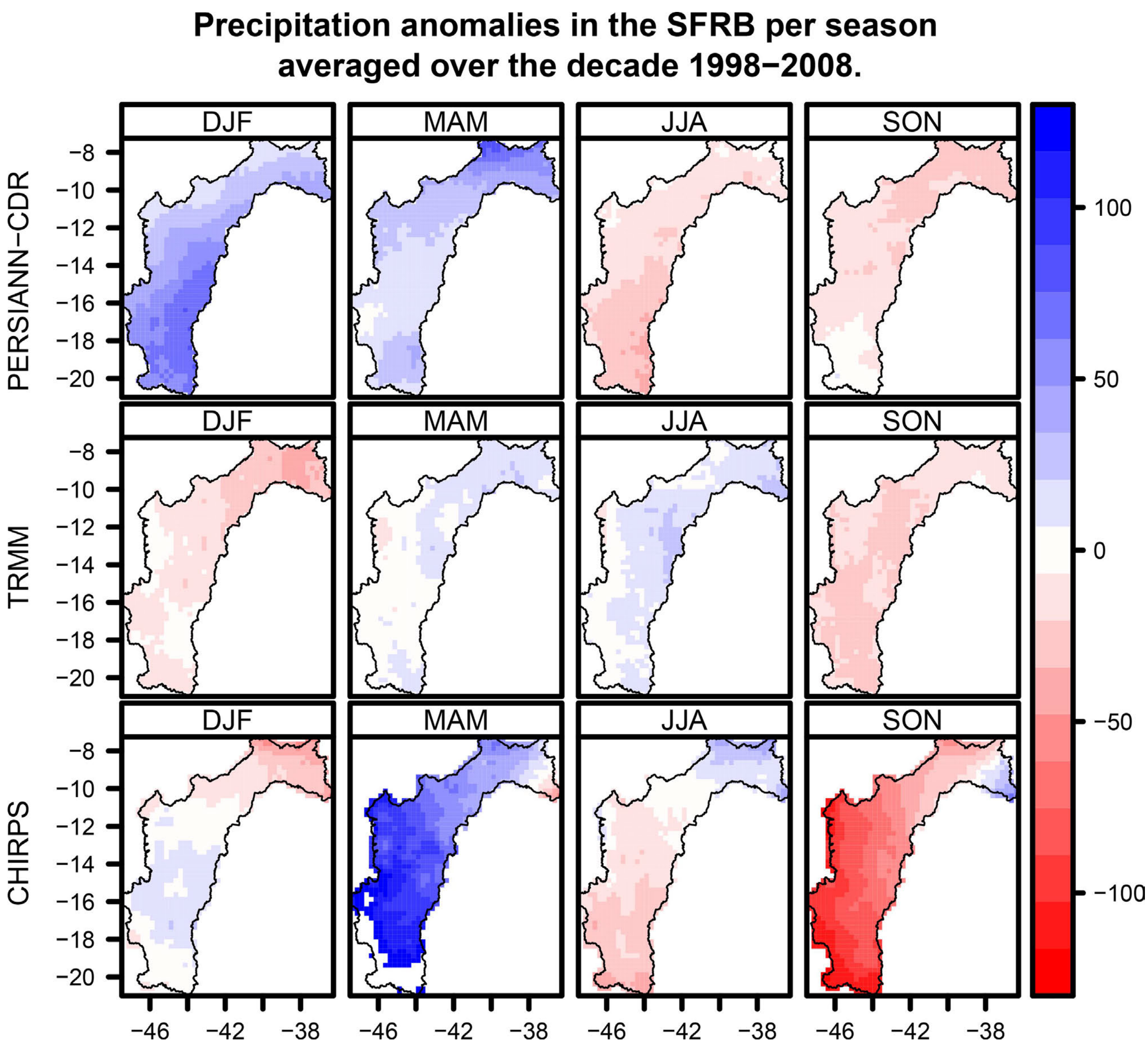

Fig. 6 - Panels with precipitation anomalies (in mm), calculated with estimates from PERSIANN-CDR, TRMM and CHIRPS, in the SFRB for D1. Each line represents the precipitation anomalies from one of the three satellite data products used in this work and each column represents the season of the year in the Southern Hemisphere, with the first column being the summer: Dec, Jan and Feb (DJF); the second column being the autumn: Mar, Apr and May (MAM); the third column being the winter: Jun, Jul and Aug (JJA); and the fourth column being the spring: Sep, Oct and Nov (SON).

values of differences in precipitation totals are largest in January and February, when it fell a little over than 25 mm and 48 mm (on average) less precipitation for D2 than it used to fall for D1. This period is characterized by the lowest precipitation amount throughout the year in the basin. The reduction in precipitation amounts is partly compensated by the increase in March and April, when it fell about 5 mm and 20 mm (on average) more precipitation for D2 than it used to fall for D1. However, the wetter autumns did not offset the even dryer summers to make the net annual balance of precipitation in the SFRB, calculated as the sum of the differences in monthly means presented in Fig. 5, to go to zero, which indicates that there was an overall decrease in precipitation in the basin from D1 to D2.

Precipitation anomalies were mapped for each season of the year and presented in panels in Fig. 6 for D1 and in Fig. 7 for D2. More extreme values in CHIRPS, which is likely to be the result of its blending process of satellite data with gauge rainfall data over a higher resolution grid (0.05 x 0.05 degrees) than TRMM or PERSIANN-CDR grids (0.25 x 0.25 degrees).

Our regional analyses of precipitation anomalies start by pointing out that anomalies vary a lot across the basin, from the upper part of the basin until the lower part of the basin. This is because the lower part of the basin is

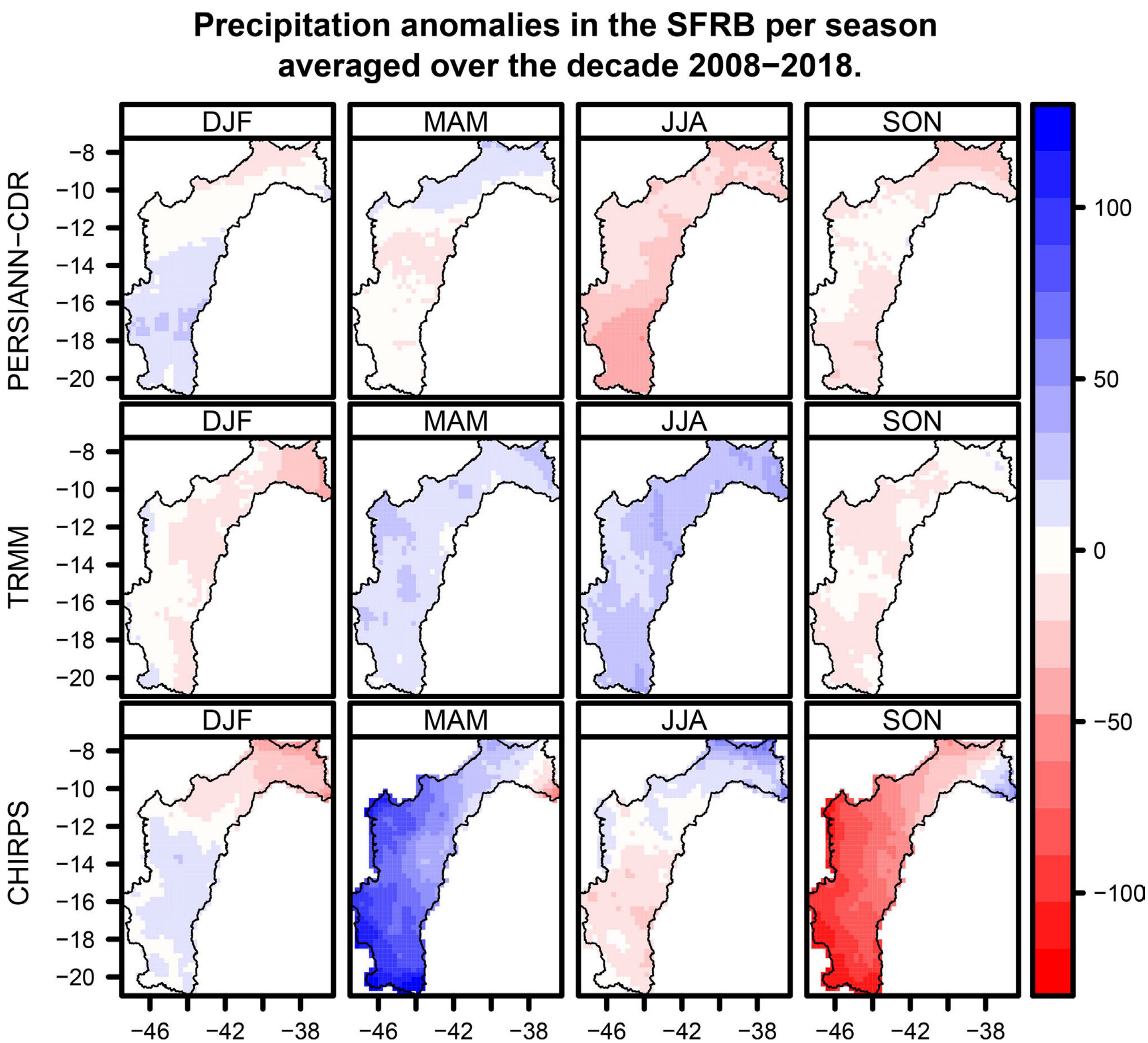

Fig. 7 - Panels with precipitation anomalies (in mm), calculated with estimates from PERSIANN-CDR, TRMM and CHIRPS, in the SFRB for D2. Each line represents the precipitation anomalies from one of the three satellite data products used in this work and each column represents the season of the year in the Southern Hemisphere, with the first column being the summer: Dec, Jan and Feb (DJF); the second column being the autumn: Mar, Apr and May (MAM); the third column being the winter: Jun, Jul and Aug (JJA); and the fourth column being the spring: Sep, Oct and Nov (SON).

within the Brazilian semiarid region (Cunha *et al.*, 2015) where precipitation amounts are usually low, especially in the summer.

The timing of the precipitation anomalies reveals that below-average precipitation occurs in the spring (i.e. SON) while above-average precipitation occurs in the autumn (i.e. mam), systematically. This pattern indicates a progressively later onset of the rainy season in the SFRB over D1 and D2. One could analyze the precipitation deficit in the SFRB based on the amount of precipitation in the middle of the rainy season, represented by the precipitation anomalies in the panels DJF. From D1 to D2, the precipitation anomalies indicate drier rainy seasons over D1 than over D2, especially for the precipitation anomalies calculated from PERSIANN-CDR. The drier rainy seasons for D2 may as well be influenced by the recent severe drought event that hit the Northeast Brazil (Marengo *et al.*, 2017).

Lastly, the correlation of drier-than-normal conditions, either in terms of 3-month SPI or precipitation deficit, highlighted in Figs. 4 and 5 was tested against the Oceanic Niña Index (ONI) and the interhemispheric SSTA gradient (GRAD) (Fig. 8). The results of the correlation analysis are shown in Fig. 9. The correlation analysis revealed that, despite the weak positive association (given by the correlation coefficient of around 0.20), the correlation between SPI and ONI and between SPI and GRAD are statistically significant at the significance level of 0.05 for dry periods in the SFRB. This result suggests that there are many factors that influence the precipitation deficit in

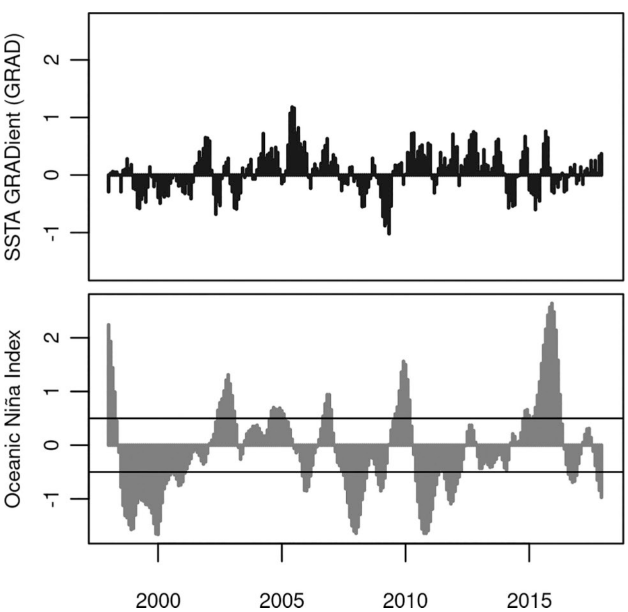

Fig. 8 - Monthly Sea surface temperature anomalies for the Pacific and Atlantic Oceans between 1998 and 2018 measured with the Oceanic Niño Index (ONI) and the interhemispheric SSTA gradient (GRAD) in °C. A threshold of ± 0.5 °C. for the Oceanic Niño Index (ONI) is drawn to identify moderate El Niño/La Niña events.

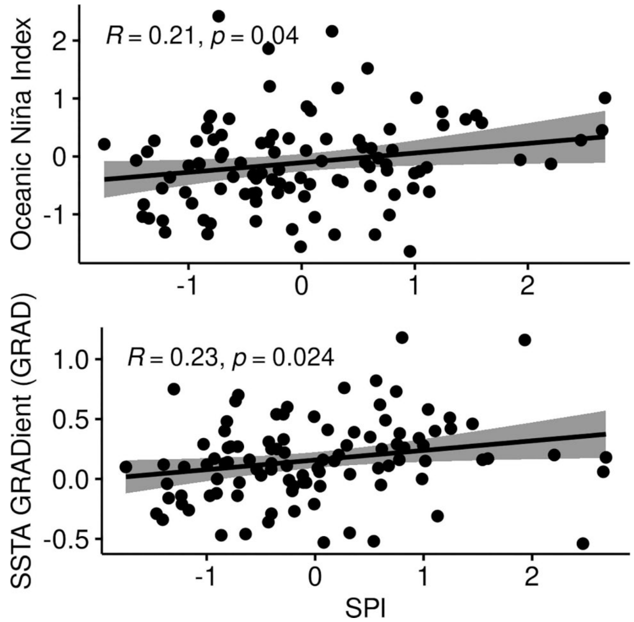

Fig. 9 - Correlation analysis of drier-than-normal conditions (as measured with SPI) in the SFRB and sea surface temperature in the Pacific Ocean and the Atlantic Ocean (as measured with ONI and GRAD).

the SFRB in the 1998-2018 period, with ONI and GRAD being one of them that are determinants. Another factors have also thought to be determinant, as for example, the result of a interdecadal variability of precipitation in the SFRB arising from inter-connections with climatic indices or sea surface temperature anomalies (Andreoli and Kayano, 2005; Grimm and Saboia, 2015).

Droughts over this region are usually explained by the El Niño-Southern Oscillation (ENSO) phenomenon, which is widely reported to cause below-average rainfall over the Northeast region of Brazil (NEB) - region that covers most of the SFRB (Jimenez *et al.*, 2021; Ambrizzi *et al.*, 2004; Coelho *et al.*, 2002). It is unlikely, however, that ENSO alone was the major factor of the precipitation deficit between D1 and the D2 for the SFRB. Instead, the precipitation deficit is thought to be a response to large scale circulation patterns of moisture transport that led to one of the most severe droughts recorded in the region, which happened to occur during D2. This drought event is discussed in more detail in Marengo *et al.* (2017); Brito *et al.* (2018); Barbosa *et al.* (2019); de Medeiros *et al.* (2020). The precipitation deficit in the SFRB and, hence, their implications has been proven to be closely linked to how the precipitation in the SFRB would respond to the combination of factors that drive the climate variability of the Brazilian semiarid.

4. Conclusion

The temporal analysis of precipitation deficit made with 3-month SPI time series revealed that the São Francisco River Basin experienced longer and drier periods in D2 than D1. Also, it has been noticed a decrease in occurrences of periods of precipitation excess and an increase in the severity of precipitation deficit from D1 to D2. Further analysis on the Mann-Kendall statistic (*S*) for the SPI time series showed that all satellite products are consistent with the negative trend in the SFRB, however the trend is statistically evident for SPI values calculated with estimates of precipitation from TRMM and PERSIANN.

Despite the changes in annual precipitation between D2 and D1 over the SFRB to be small, our seasonal analysis showed that decadal changes in precipitation totals were significant during the summer, when precipitation amounts were lower for D2 than D1. Combined with the regional analysis, this reduction in precipitation amounts in the summer was more relevant in the upper part of the SFRB, where a wetter climate - compared to the overall climate in the SFRB - strongly influenced by El Niño/ Southern Oscillation-related precipitation takes place.

Authors' contributions

Data collection and data processing were performed by José Damasceno and Erick Oliveira. Formal analysis and investigation were performed by Fábio Pereira. The approach used to assess the droughts in SFRB was pointed out by Fábio Pereira and Zheng Duan. The first draft of the manuscript was written by Fábio Pereira.

Conflict of interest

All authors certify that they have no affiliations with or involvement in any organization or entity with any financial interest or non-financial interest in the subject matter or materials discussed in this manuscript.

Acknowledgments

The authors are grateful to Fundação de Amparo à Pesquisa do Estado de Alagoas (FAPEAL) for providing travel grants to discuss the insights and the work presented in this manuscript with other researchers at Lund University. We also thank Prof Duan Zheng from Lund University for the fruitful feedback provided to this work. Erick Oliveira received a stipend for young investigators from Programa Institucional de Bolsas de Iniciação Científica (PIBIC) granted by Universidade Federal de Alagoas (UFAL). We are also grateful to Fundação de Amparo à Pesquisa do Estado de Alagoas (FAPEAL) for the travel grant offered to the authors through the ERC - CONFAP - CNPq Call for Research opportunities in Europe for active PhD researchers from Brazil, which could enrich the work by presenting its bottom line and discussing its outcomes with researchers and peers from all over the world in workshops and seminars at Lund University.

References

ALIJANIAN, M.; RAKHSHANDEHROO, G.R.; DEHGHANI, M.; MISHRA, A. Probabilistic drought forecasting using copula and satellite rainfall based PERSIANN-CDR and MSWEP datasets. **International Journal of Climatology**, v. 42, n. 12, 2022.

AMBRIZZI, T.; SOUZA, E.B.D.; PULWARTY, R.S. The Hadley and walker regional circulations and associated ENSO impacts on south American seasonal rainfall. **The Hadley Circulation: Present, Past and Future**. New York: Springer, p. 203-235, 2004.

ANA. **Conjuntura dos Recursos Hídricos no Brasil: 2013 - Tech. Rep**. Brasília: Agência Nacional de Águas, 2013. Disponível em https://arquivos.ana.gov.br/institucional/spr/conjuntura/ANA_Conjuntura_Recursos_Hidricos_Brasil/ANA_Conjuntura_Recursos_Hidricos_Brasil_2013_Final.pdf.

ANDREOLI, R.V.; KAYANO, M.T. ENSO-related rainfall anomalies in South America and associated circulation features during warm and cold Pacific decadal oscillation regimes. **International Journal of Climatology**, v. 15, n. 15, p. 2017-2030, 2005. doi

ANDREOLI, R.V.; KAYANO, M.T. A importância relativa do atlântico tropical sul e pacífico leste na variabilidade de precipitação do nordeste do brasil. **Revista Brasileira de Meteorologia**, v. 22, n. 1, p. 63-74, 2007.

BARBOSA, H.A.; KUMAR, T.L.; PAREDES, F.; ELLIOTT, S.; AYUGA, J. Assessment of caatinga response to drought using meteosat-seviri normalized difference vegetation index (2008-2016). **ISPRS Journal of Photogrammetry and Remote Sensing**, v. 148, p. 235-252, 2019.

BEZERRA, B.G.; SILVA, L.L.; SANTOS E SILVA, C.M.; DE CARVALHO, G.G. Changes of precipitation extremes indices in São Francisco River Basin, Brazil from 1947 to 2012. **Theoretical and Applied Climatology**, n. 135, p. 565-576, 2019. doi

BRASIL. **Projeto de Integração do Rio São Francisco com Bacias Hidrográficas do Nordeste Setentrional. Relatório de Impacto Ambiental - RIMA**. Brasília: Ministério do Desenvolvimento Regional, 2004. Disponível em https://antigo.mdr.gov.br/images/stories/ProjetoRioSaoFrancisco/ArquivosPDF/documentostecnicos/RIMA JULHO2004.pdf.

BRASIL NETO, R.M.; SANTOS, C.A.G.; SILVA, J.F.C.B.C.; DA SILVA, R.M.; DOS SANTOS, C.A.C.; MISHRA, M. Evaluation of the TRMM product for monitoring drought over Paraíba State, northeastern Brazil: a trend analysis. **Scientific Reports**, v. 11, n. 1097, p. 1-18, 2021. doi

BRITO, S.S.B.; CUNHA, A.P.M.; CUNNINGHAM, C.; ALVALÁ, R.C.; MARENGO, J.A.; CARVALHO, M.A. Frequency, duration and severity of drought in the semiarid northeast brazil region. **International Journal of Climatology**, v. 38, n. 2, p. 517-529, 2018.

CHESF. **Relatorio Anual 2020. Tech. Rep**. Recife: Companhia Hidro Elétrica do São Francisco, 2020. Disponível em https://www.chesf.gov.br/sustentabilidade/Documents/Relatorio_Anual_2020.pdf.

CHO, H.K.; BOWMAN, K.P.; NORTH, G.R. A comparison of gamma and lognormal distributions for characterizing satellite rain rates from the tropical rainfall measuring mission. **Journal of Applied Meteorology**, n. 11, p. 1586-1597, 2004.

COELHO, C.A.S.; UVO, C.B.; AMBRIZZI, T. Exploring the impacts of the tropical pacific SST on the precipitation patterns over South America during ENSO periods. **Theoretical and Applied Climatology**, v. 71, n. 3, p. 185-197, 2002.

COUTINHO, P.E.; CATALDI, M. Assessment of water availability in the period of 100 years at the head of the São Francisco River basin, based on climate change scenarios. **Revista Engenharia na Agricultura - Reveng**, v. 29, p. 107-121, 2021. doi

CUNHA, A.P.M.; ALVALÁ, R.C.; NOBRE, C.A.; CARVALHO, M.A. Monitoring vegetative drought dynamics in the Brazilian semiarid region. **Agricultural and Forest Meteorology**, v. 214-215, p. 494-505, 2015. doi

DE PAIVA, L.F.G.; MONTENEGRO, S.M.; CATALDI, M. Prediction of monthly flows for Três Marias reservoir (São Francisco River basin) using the CFS climate forecast model. **Revista Brasileira de Recursos Hídricos**, v. 25, p. E16, 2020. doi

DE SOUZA, E.; KAYANO, M.T.; AMBRIZZI, T. Intraseasonal and submonthly variability over the eastern amazon and northeast brazil during the autumn rainy season. **Theoretical and Applied Climatology**, v. 81, n. 3, p. 177-191, 2005.

ESIT, M.; KUMAR, S.; PANDEY, A.; LAWRENCE, D.M.; RANGWALA, I.; YEAGER, S. Seasonal to multi-year soil moisture drought forecasting. **Climate and Atmospheric Science**, v. 4, n. 16, p. 1-8, 2021. doi

FERREIRA, D.B.; BARROSO, G.R.; DANTAS, M.S.; OLIVEIRA, K.L.; CHRISTOFARO, C.; OLIVEIRA, S.C. Pluviometric patterns in the São Francisco River basin in Minas Gerais, Brazil. **Revista Brasileira de Recursos Hídricos**, v. 26, p. E27, 2021. doi

FUNK, C.; PETERSON, P.; LANDSFELD, M.; PEDREROS, D.; VERDIN, J.; *et al.* The climate hazards infrared precipitation with stations - A new environmental record for monitoring extremes. **Scientific Data**, v. 2, n. 1, p. 150066, 2015. doi

GAO, F.; ZHANG, Y.; REN, X.; YAO, Y.; HAO, Z.; CAI, W. Evaluation of chirps and its application for drought monitoring over the haihe river basin, China. **Natural Hazards**, v. 92, n. 1, p. 155-172, 2018. doi

GRIMM, A.M.; SABOIA, J.P.J. Interdecadal Variability of the South American precipitation in the monsoon season. **Journal of Climate**, v. 28, n. 2, p. 755-775, 2015. doi

HAZELL, P.; WOOD, S. Drivers of change in global agriculture. **Philosophical Transactions of the Royal Society B: Biological Sciences**, v. 363, n. 1491, p. 495-515, 2008. doi

JIMENEZ, J.C.; MARENGO, J.A.; ALVES, L.M.; SULCA, J.C.; TAKAHASHI, K.; *et al.* The role of enso flavours and tna on recent droughts over amazon forests and the northeast brazil region. **International Journal of Climatology**, v. 41, n. 7, p. 3761-3780, 2021.

DE JONG, P.; TANAJURA, C.A.S.; SÁNCHEZ, A.S.; DARGAVILLE, R.; KIPERSTOK, A.; TORRES, E.A. Hydroelectric production from Brazil's São Francisco River could cease due to climate change and inter-annual variability. **Science of The Total Environment**, v. 634, p. 1540-1553, 2018. doi

KAYANO, M.T.; ANDREOLI, R.V. Relationships between rainfall anomalies over northeastern brazil and the El Niño-southern oscillation. **Journal of Geophysical Research: Atmospheres**, v. 111, n. D13, 2006.

LAI, C.; ZHONG, R.; WANG, Z.; WU, X.; CHEN, X.; *et al.* Monitoring hydrological drought using long-term satellite-based precipitation data. **Science of the Total Environment**, v. 649, p. 1198-1208, 2019.

LUCAS, M.C.; KUBLIK, N.; RODRIGUES, D.B.B.; MEIRA NETO, A.A.; ALMAGRO, A.; *et al.* Significant baseflow reduction in the São Francisco River Basin. **Water**, v. 13, n. 1, p. 2, 2021. doi

MANETA, M.; TORRES, M.; VOSTI, S.A.; WALLENDER, W.W.; ALLEN, S.; *et al.* Assessing agriculture-water links at the basin scale: Hydrologic and economic models of the São Francisco River Basin, Brazil. **Water International**, v. 34, n. 1, p. 88-103, 2009a. doi

MANETA, M.P.; TORRES, M.; WALLENDER, W.W.; VOSTI, S.; KIRBY, M.; *et al.* Water demand and flows in the São Francisco River Basin (Brazil) with increased irrigation. **Agricultural Water Management**, v. 96, n. 8, p. 1191-1200, 2009b. doi

MARENGO, J.A.; CHOU, S.C.; KAY, G.; ALVES, L.M.; PESQUERO, J.F.; *et al.* Development of regional future climate change scenarios in South America using the Eta CPTEC/HadCM3 climate change projections: climatology and regional analyses for the Amazon, São Francisco and the Paraná River basins. **Climate Dynamics**, v. 38, n. 9, p. 1829-1848, 2012. doi

MARENGO, J.A.; ALVES, L.M.; ALVALA, R.; CUNHA, A.P.; BRITO, S.; MORAES, O.L. Climatic characteristics of the 2010-2016 drought in the semiarid northeast brazil region. **Anais da Academia Brasileira de Ciências**, v. 90, n. 2, p. 1973-1985, 2017.

MARQUES, R.F.C.; OYAMA, M.D. Interannual variability of precipitation for the centro de lançamento de Alcântara in enso-neutral years. **Journal of Aerospace Technology and Management**, v. 7, n. 3, p. 365-373, 2015.

DE MEDEIROS, F.J.; DE OLIVEIRA, C.P.; TORRES, R.R. Climatic aspects and vertical structure circulation associated with the severe drought in Northeast Brazil (2012-2016). **Climate Dynamics**, v. 55, n. 9, p. 2327-2341, 2020.

MUN, Y.S.; NAM, W.H.; JEON, M.G.; KIM, T.; HONG, E.M.; *et al.* Application of meteorological drought index using climate hazards group infrared precipitation with station (chirps) based on global satellite-assisted precipitation products in Korea. **Journal of the Korean Society of Agricultural Engineers**, v. 61, n. 2, p. 1-11, 2019.

OLIVEIRA, P.T.S.; NEARING, M.A.; MORAN, M.S.; GOODRICH, D.C.; WENDLAND, E.; GUPTA, HV. Trends in water balance components across the Brazilian Cerrado. **Water Resources Research**, v. 50, n. 9, p. 7100-7114, 2014. doi

RODRIGUES, R.R.; HAARSMA, R.J.; CAMPOS, E.J.; AMBRIZZI, T. The impacts of inter-El Niño variability on the tropical Atlantic and northeast Brazil climate. **Journal of Climate**, v. 24, n. 13, p. 3402-3422, 2011.

SANDEEP, P.; REDDY, G.O.; JEGANKUMAR, R.; KUMAR, K.A. Monitoring of agricultural drought in semi-arid ecosystem of peninsular India through indices derived from time-series chirps and MODIS datasets. **Ecological Indicators**, v. 121, p. 107033, 2021.

SANTOS, C.A.G.; DE MORAIS, B.S. Identification of precipitation zones within São Francisco River basin (Brazil) by global wavelet power spectra. **Hydrological Sciences Journal**, v. 58, n. 4, p. 789-796, 2013. doi

SANTOS, C.A.G.; BRASIL NETO, R.M.; PASSOS, J.S.A.; DA SILVA, R.M. Drought assessment using a TRMM-derived standardized precipitation index for the upper São Francisco River basin, Brazil. **Environmental Monitoring and Assessment**, v. 189, n. 6, p. 250, 2017. doi

SANTOS, C.A.G.; BRASIL NETO, R.M.; DA SILVA, R.M.; PASSOS, J.S.A. Integrated spatiotemporal trends using TRMM 3B42 data for the Upper São Francisco River basin, Brazil. **Environmental Monitoring and Assessment**, v. 190, n. 3, p. 175, 2018. doi

SANTOS, C.A.G.; NETO R.M.B.; DO NASCIMENTO, T.V.M.; DA SILVA, R.M.; MISHRA, M.; FRADE, T.G. Geospatial drought severity analysis based on PERSIANN-CDR-estimated rainfall data for Odisha state in India (1983-2018). **Science of The Total Environment**, v. 750, p. 141258, 2021.

DA SILVA, M.V.M.; SILVEIRA, C.S.; COSTA, J.M.F.; MARTINS, E.S.P.R.; VASCONCELOS JUNIOR, F.C. Projection of Climate Change and Consumptive Demands Projections Impacts on Hydropower Generation in the São Francisco River Basin, Brazil. **Water**, v. 13, n. 3, p. 332, 2021. doi

ALVES DA SILVA ROSA, L.; MORAIS, M.; SAITO, C.H. Water security and river basin revitalization of the São Francisco River Basin: A symbiotic relationship. **Water**, v. 13, n. 7, p. 907, 2021. doi

SOUTO, J.; BELTRÃO, N.; TEODORO, A. Performance of remotely sensed soil moisture for temporal and spatial analysis of rainfall over São Francisco River Basin, Brazil. **Geosciences**, v. 9, n. 3, p. 144, 2019. doi

SU, F.; HONG, Y.; LETTENMAIER, D.P. Evaluation of TRMM Multisatellite Precipitation Analysis (TMPA) and its utility in hydrologic prediction in the La Plata Basin. **Journal of Hydrometeorology**, v. 9, n. 4, p. 622-640, 2008. doi

SUN, T.; FERREIRA, V.G.; HE X.; ANDAM-AKORFUL, S.A. Water availability of São Francisco River Basin based on a space-borne geodetic sensor. **Water**, v. 8, n. 5, p. 213, 2016. doi

TORRES, M.O.; MANETA, M.; HOWITT, R.; VOSTI, S.A.; WALLENDER, W.W.; *et al.* Economic impacts of regional water scarcity in the São Francisco River Basin, Brazil: An application of a linked hydro-economic model. **Environment and Development Economics**, v. 17, n. 2, p. 227-248, 2012. doi

TREJO, F.P.; BRITO-CASTILLO, L.; ALVES, H.B.; GUEVARA, E. Main features of large-scale oceanic-atmospheric circulation related to strongest droughts during rainy season in Brazilian São Francisco River Basin. **International Journal of Climatology**, v. 36, n. 12, p. 4102-4117, 2016. doi

ZHONG, R.; CHEN, X.; LAI, C.; WANG, Z.; LIAN, Y.; *et al.* Drought monitoring utility of satellite-based precipitation products across mainland China. **Journal of Hydrology**, v. 568, p. 343-359, 2019. doi

Internet Resources

Physical Sciences Laboratory Database: https://psl.noaa.gov/data/climateindices/.